How good is the bipolar approximation of active regions for surface flux transport?

Anthony Yeates

COFFIES seminar, 12-Jan-2021

Motivation

- The **surface flux transport** (**SFT**) model is remarkably effective at mimicking the large-scale decay of active region magnetic fields.
  [cf. Jiang et al., *Space Sci Rev* 2014; Wang, *Space Sci Rev* 2017]

- Current interest:
  - Making solar cycle predictions before the end of the previous cycle.
  - Driving continuous simulations of the coronal magnetic field.

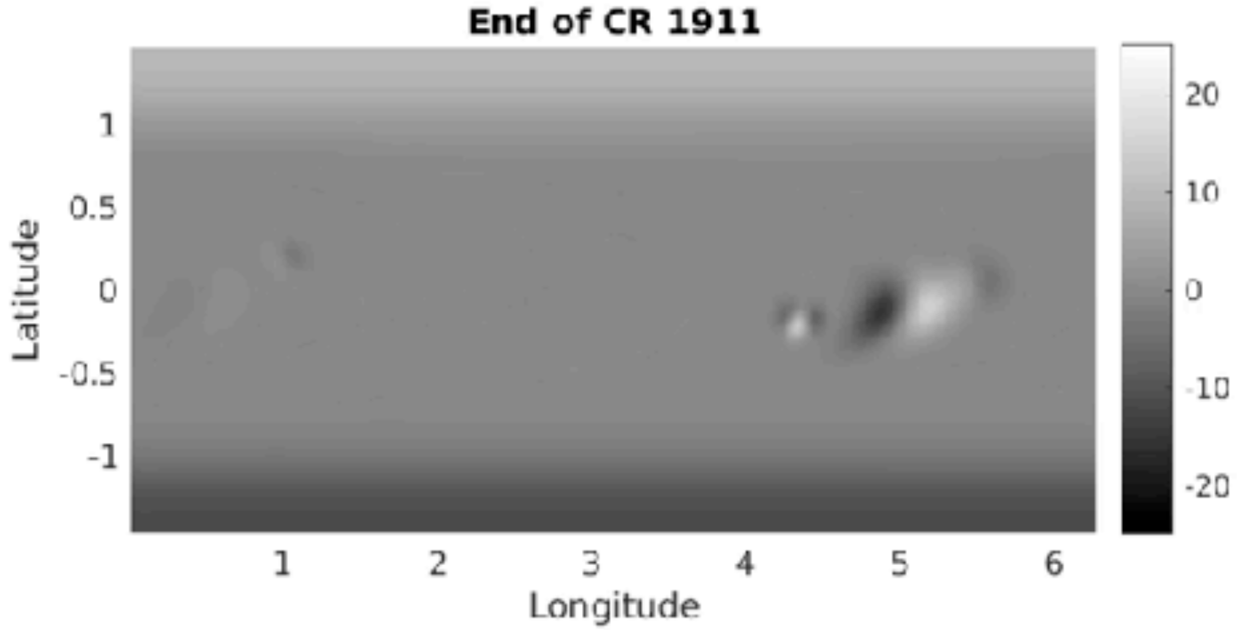

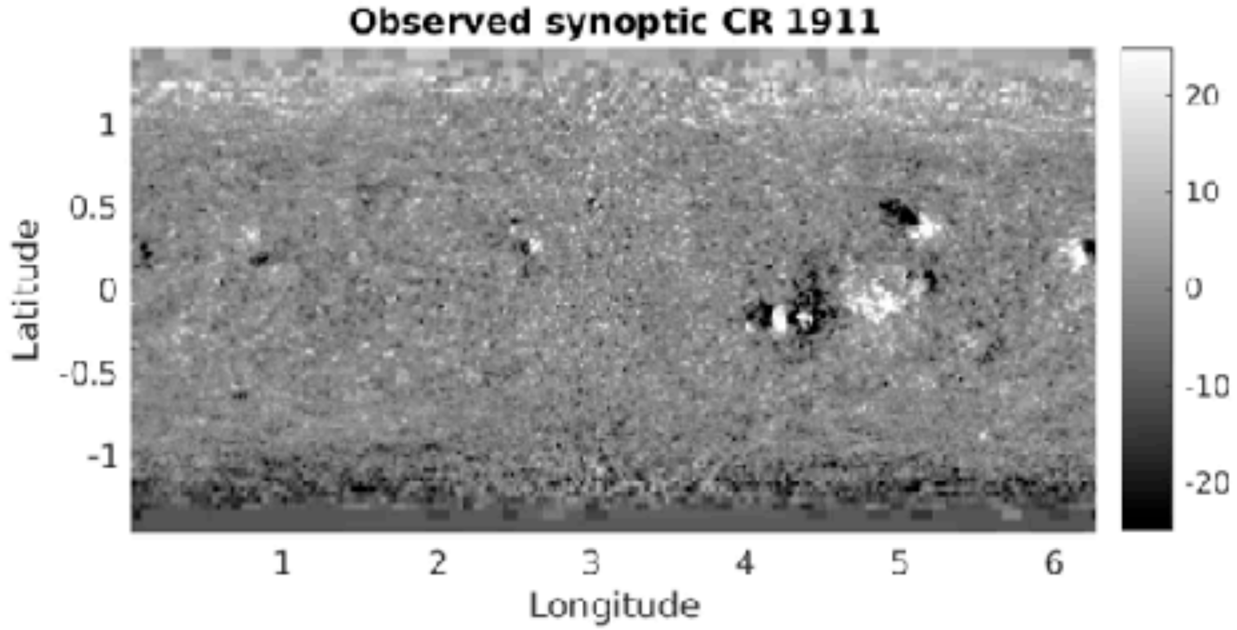

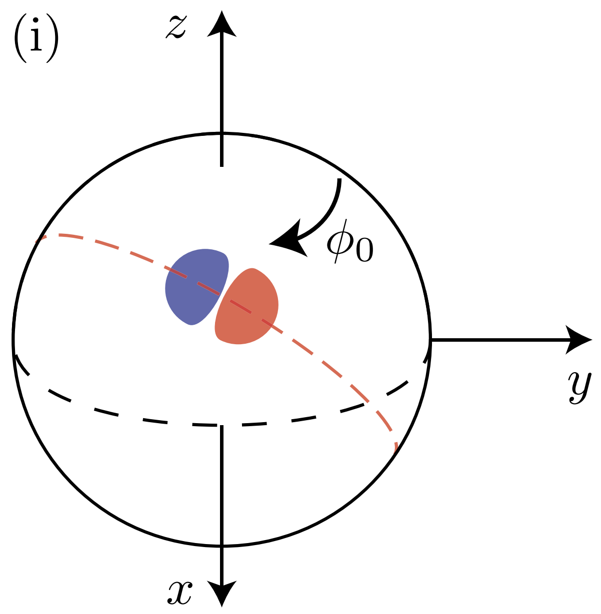

What is lost by the traditional assumption of symmetric bipolar magnetic sources?

Leading/following asymmetry

- Following polarities are often more diffuse.
- Iijima-Hotta-Imada 2019 -
  SFT simulations to investigate the effect (tilt angle proportional to latitude, all same asymmetry).
- Accounting for asymmetry weakens dipole and gives better reversal time.

(a) Effect of tilt angle

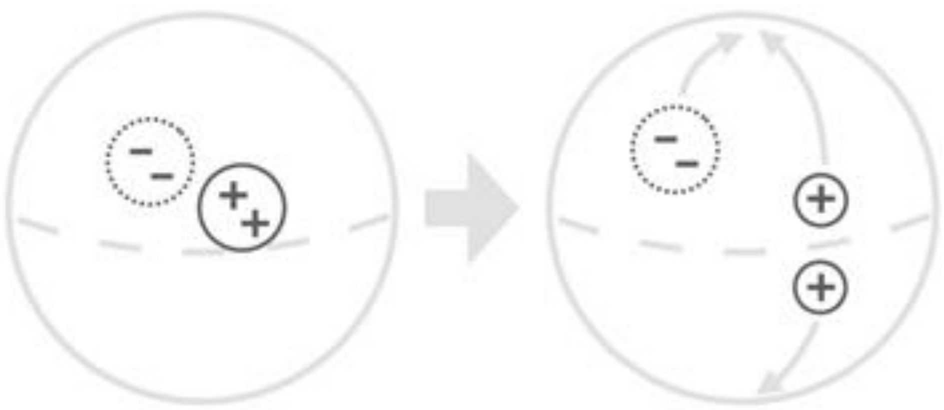

(b) Effect of size asymmetry

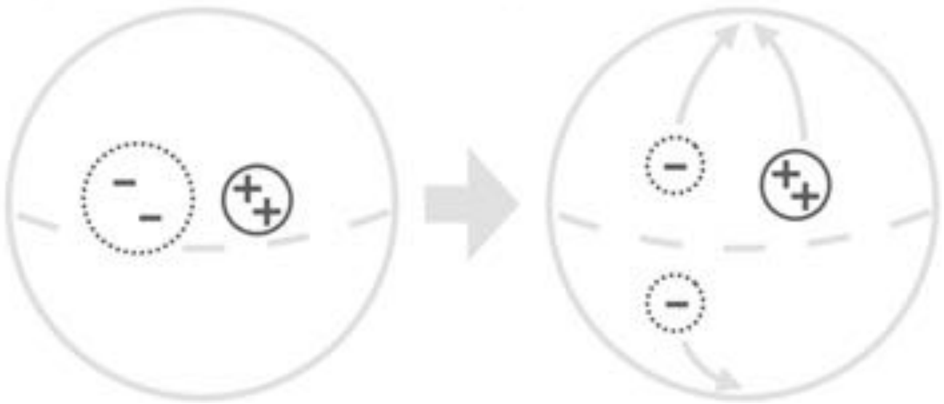

area ratio 1.0

area ratio 0.4

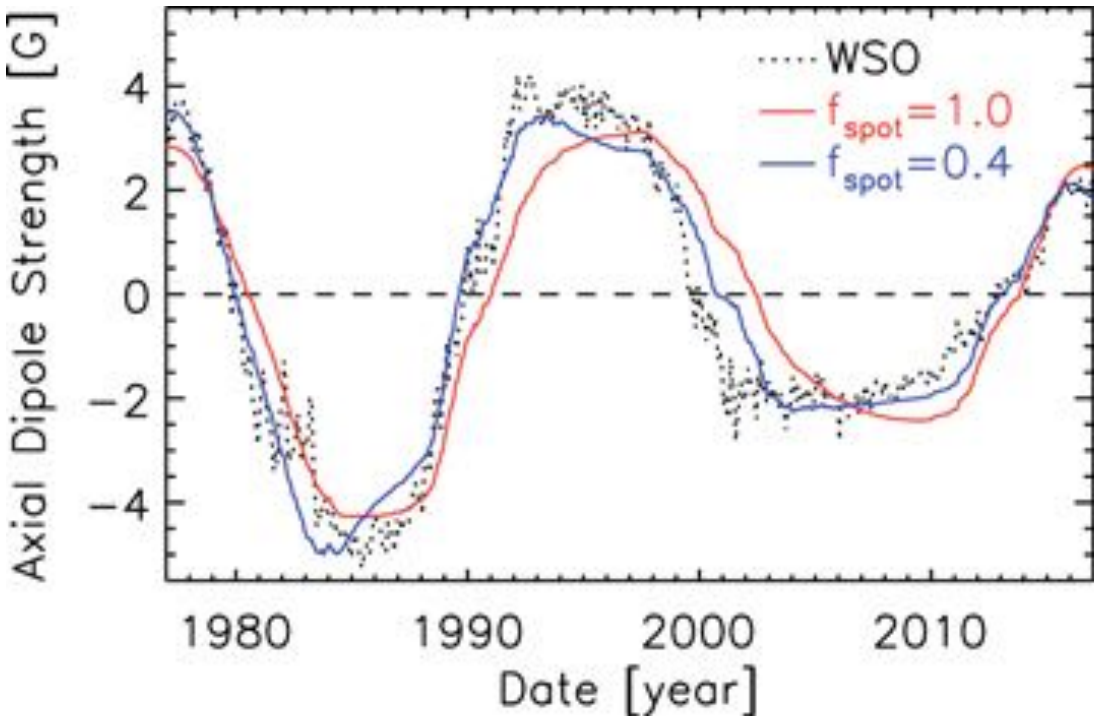

Complexity

- Jiang et al. 2019 -
  case studies of SFT evolution for two active regions.

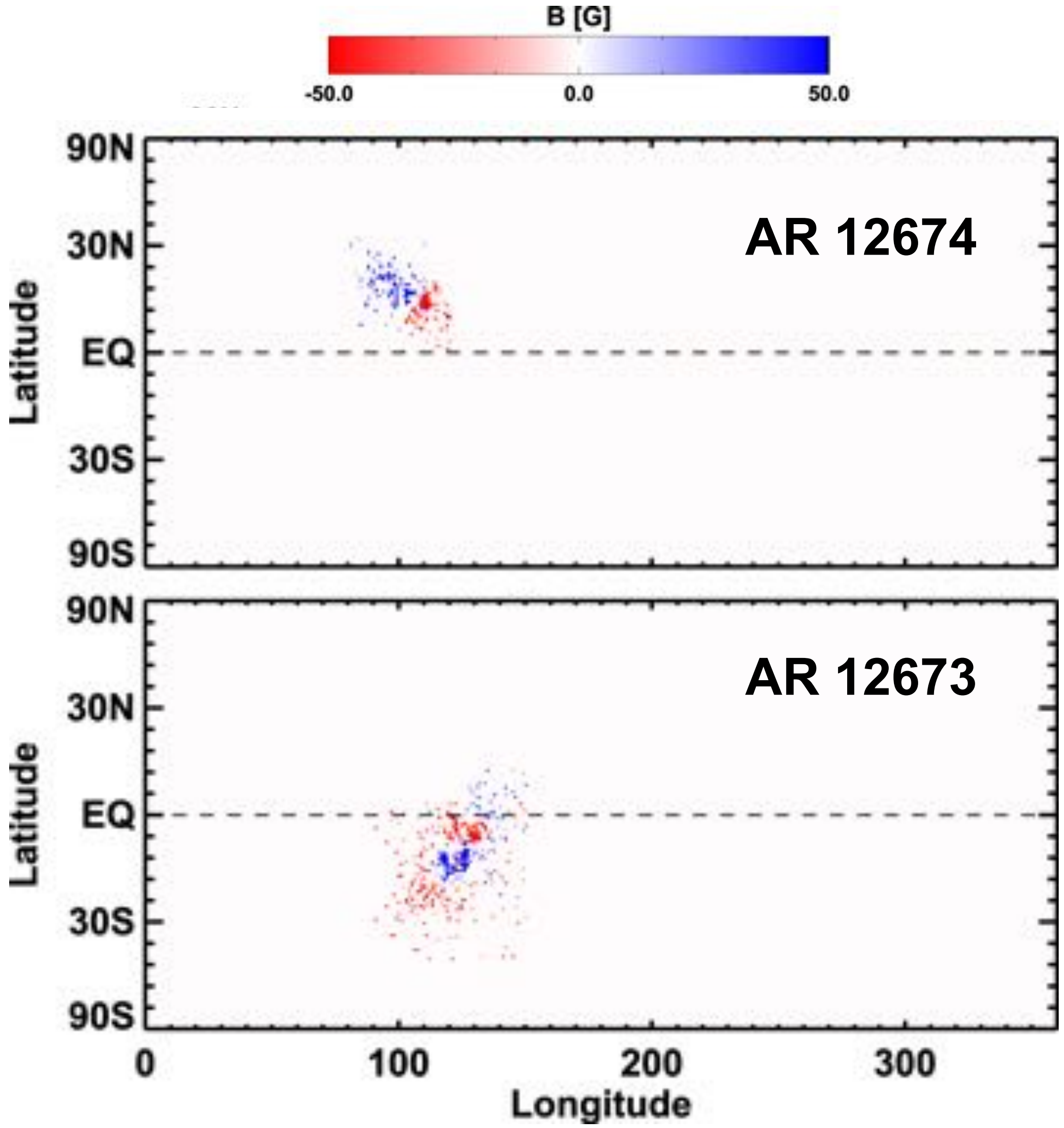

- Axial dipole changes sign for the more complex region.

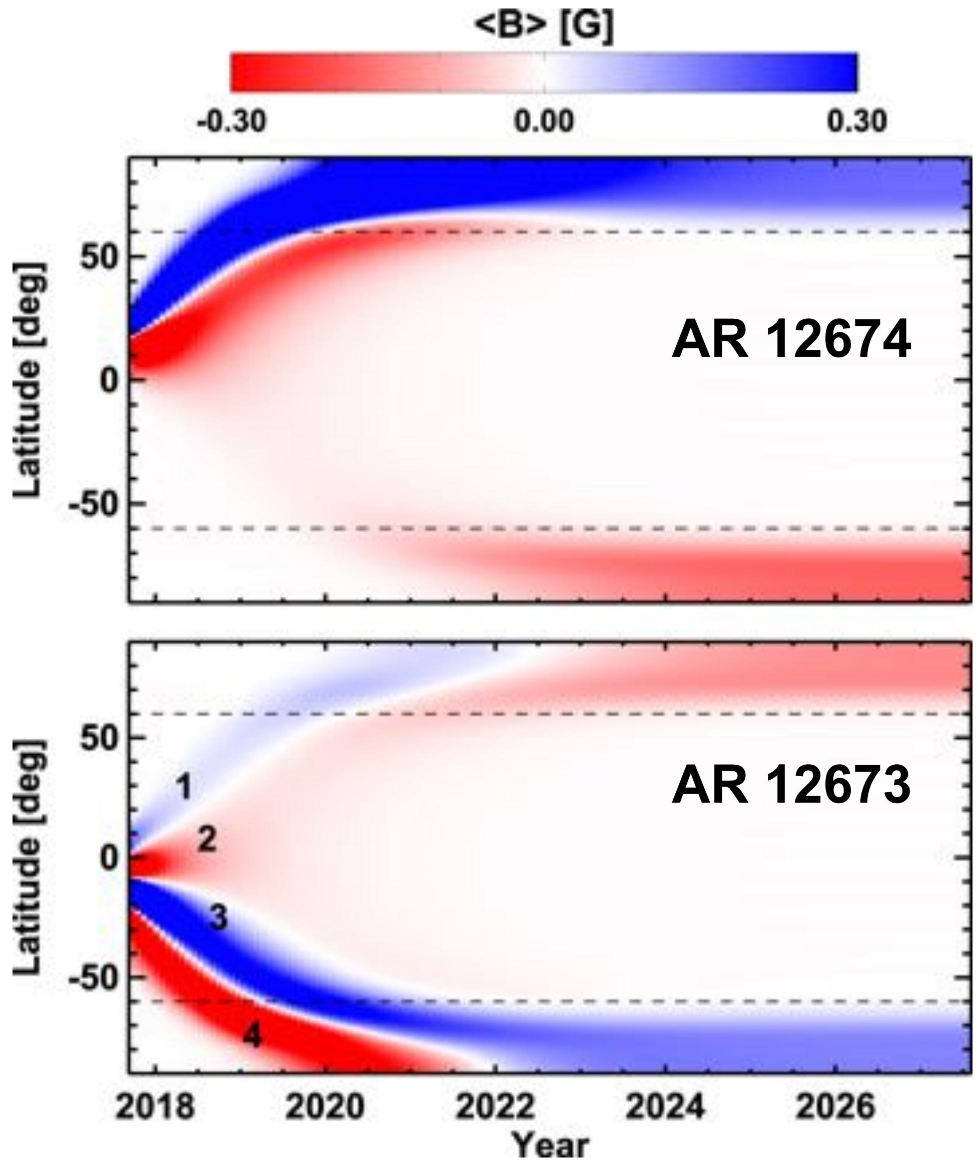

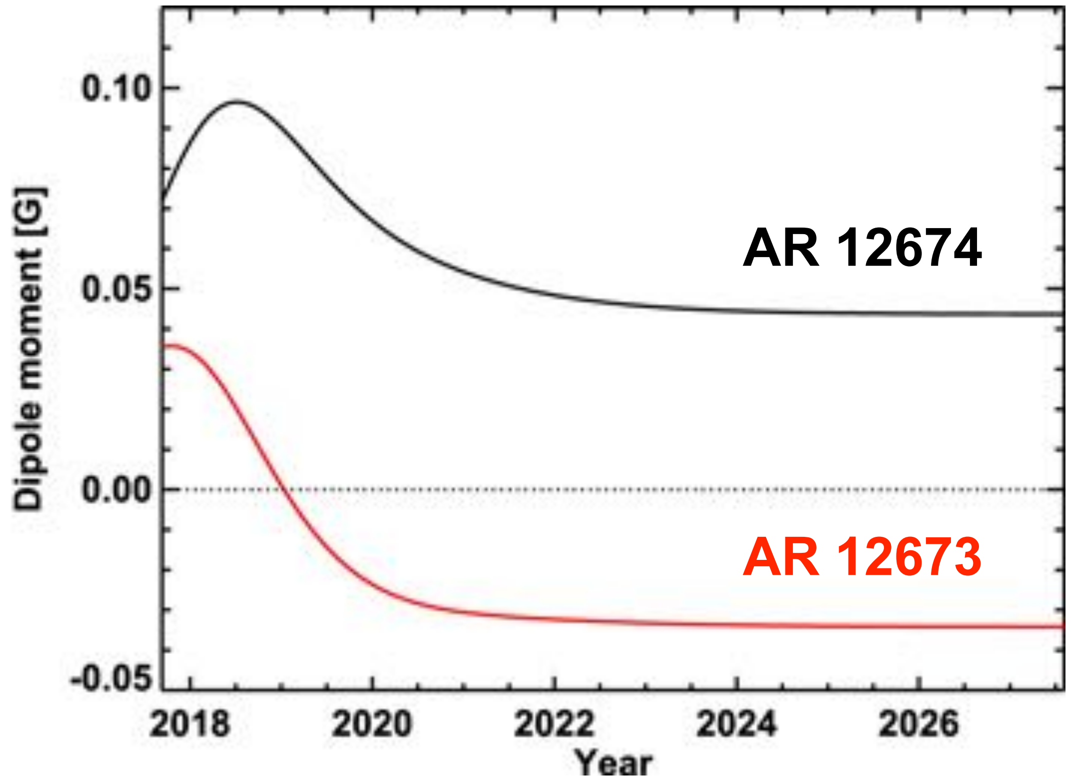

My work

- Automated database of Bipolar Magnetic Regions from HMI/SHARPs.
- Compare SFT models with BMRs vs original SHARPs.

A.R. Yeates, How good is the bipolar approximation of active regions for surface flux transport?, *Solar Physics* **295**, 119 (2020)

- Python code for extracting database: https://github.com/antyeates1983/sharps-bmrs
- Ready-prepared file: https://doi.org/10.7910/DVN/1Z7YMT (Harvard Dataverse) for **May 2010 to April 2020**:

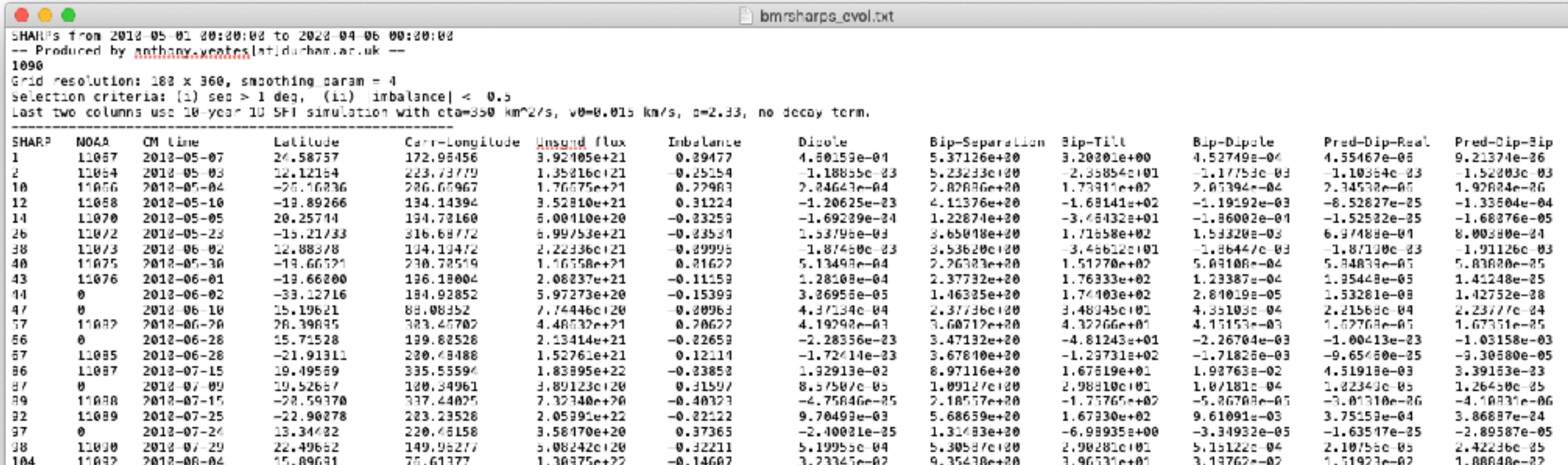

```
SHARPs from 2010-05-01 00:00:00 to 2020-04-06 00:00:00
-- Produced by anthony.yeates[at]durham.ac.uk --
1090
Grid resolution: 180 x 360, smoothing_param = 4
Selection criteria: (i) sep > 1 deg,  (ii) |imbalance| <  0.5
Last two columns use 10-year 1D SFT simulation with eta=350 km^2/s, v0=0.015 km/s, p=2.33, no decay term.
-------------------------------------------------------------
SHARP   NOAA    CM time     Latitude     Carr-Longitude  Unsgnd flux   Imbalance   Dipole        Bip-Separation  Bip-Tilt      Bip-Dipole    Pred-Dip-Real  Pred-Dip-Bip
1       11067   2010-05-07  24.58757     172.96456       3.92405e+21    0.09477    4.60159e-04   5.37126e+00     3.20801e+00   4.52749e-04   4.55467e-06    9.21374e-06
2       11064   2010-05-03  12.12164     223.73779       1.35816e+21   -0.25154   -1.18855e-03   5.23233e+00    -2.35854e+01  -1.17753e-03  -1.10364e-03   -1.52803e-03
10      11066   2010-05-04  -25.16836    286.66967       1.76675e+21    0.22983    2.04643e-04   2.02886e+00     1.73311e+02   2.05394e-04   2.34538e-06    1.92884e-06
12      11068   2010-05-10  -19.89266    134.14394       3.52810e+21    0.31224   -1.20625e-03   4.11376e+00    -1.68141e+02  -1.19192e-03  -8.52827e-05   -1.33504e-04
14      11070   2010-05-05  20.25744     194.78160       6.00410e+20   -0.03259   -1.69289e-04   1.22874e+00    -3.46432e+01  -1.06002e-04  -1.52582e-05   -1.68876e-05
26      11072   2010-05-23  -15.21733    316.68772       6.99753e+21   -0.03534    1.53796e-03   3.65048e+00     1.71658e+02   1.53320e-03   6.97488e-04    8.00380e-04
38      11073   2010-06-02  12.88378     194.19472       2.22336e+21   -0.09996   -1.87460e-03   3.53620e+00    -3.46612e+01  -1.86447e-03  -1.87190e-03   -1.91126e-03
40      11075   2010-05-30  -19.66321    230.78519       1.16558e+21    0.01622    5.13498e-04   2.26383e+00     1.51270e+02   5.03108e-04   5.84839e-05    5.83880e-05
43      11076   2010-06-01  -19.66200    196.18004       2.08237e+21   -0.11159    1.28108e-04   2.37732e+00     1.76333e+02   1.23387e-04   1.35448e-05    1.41248e-05
44      0       2010-06-02  -33.12716    184.92852       5.97273e+20   -0.15399    3.06956e-05   1.46385e+00     1.74403e+02   2.84019e-05   1.53281e-08    1.42752e-08
47      0       2010-06-10  15.19621     88.08352        7.74446e+20   -0.00963    4.37134e-04   2.37736e+00     3.48345e+01   4.35103e-04   2.21568e-04    2.23777e-04
57      11082   2010-06-20  28.39835     303.46702       4.48632e+21    0.20622    4.19298e-03   3.60712e+00     4.32266e+01   4.15153e-03   1.62768e-05    1.67351e-05
66      0       2010-06-28  15.71528     139.82528       2.13414e+21   -0.02659   -2.28356e-03   3.47132e+00    -4.81243e+01  -2.26704e-03  -1.00413e-03   -1.03158e-03
67      11085   2010-06-28  -21.91311    280.48488       1.52761e+21    0.12114   -1.72414e-03   3.67840e+00    -1.29731e+02  -1.71826e-03  -9.65460e-05   -9.30680e-05
86      11087   2010-07-15  19.49569     335.55594       1.83895e+22   -0.03858    1.32913e-02   8.97116e+00     1.67619e+01   1.98763e-02   4.51918e-03    3.39163e-03
87      0       2010-07-09  19.52667     180.34961       3.89123e+20    0.31597    8.57507e-05   1.09127e+00     2.98810e+01   1.07181e-04   1.82349e-05    1.26450e-05
89      11088   2010-07-15  -20.59370    337.44025       7.32340e+20   -0.40323   -4.75846e-05   2.18537e+00    -1.75765e+02  -5.86708e-05  -3.01310e-06   -4.10831e-06
92      11089   2010-07-25  -22.90278    203.23528       2.05391e+22   -0.02122    9.70493e-03   5.68659e+00     1.67330e+02   9.61091e-03   3.75153e-04    3.86887e-04
97      0       2010-07-24  13.34482     220.46158       3.58470e+20    0.37365   -2.40081e-05   1.31483e+00    -6.98935e+00  -3.34932e-05  -1.63547e-05   -2.89587e-05
98      11090   2010-07-29  22.49662     149.96277       5.08242e+20   -0.32211    5.19955e-04   5.30587e+00     2.90281e+01   5.15122e-04   2.10756e-05    2.42236e-05
104     11092   2010-08-04  15.89631     75.61377        1.30375e+22   -0.14607    3.23345e-02   9.35430e+00     3.96531e+01   3.13762e-02   1.51923e-02    1.80840e-02
```

Building the Database

SHARP data

http://jsoc.stanford.edu/doc/data/hmi/sharp/sharp.htm

- I use `hmi.sharp_cea_720s` — “definitive” data (after full-disk package).

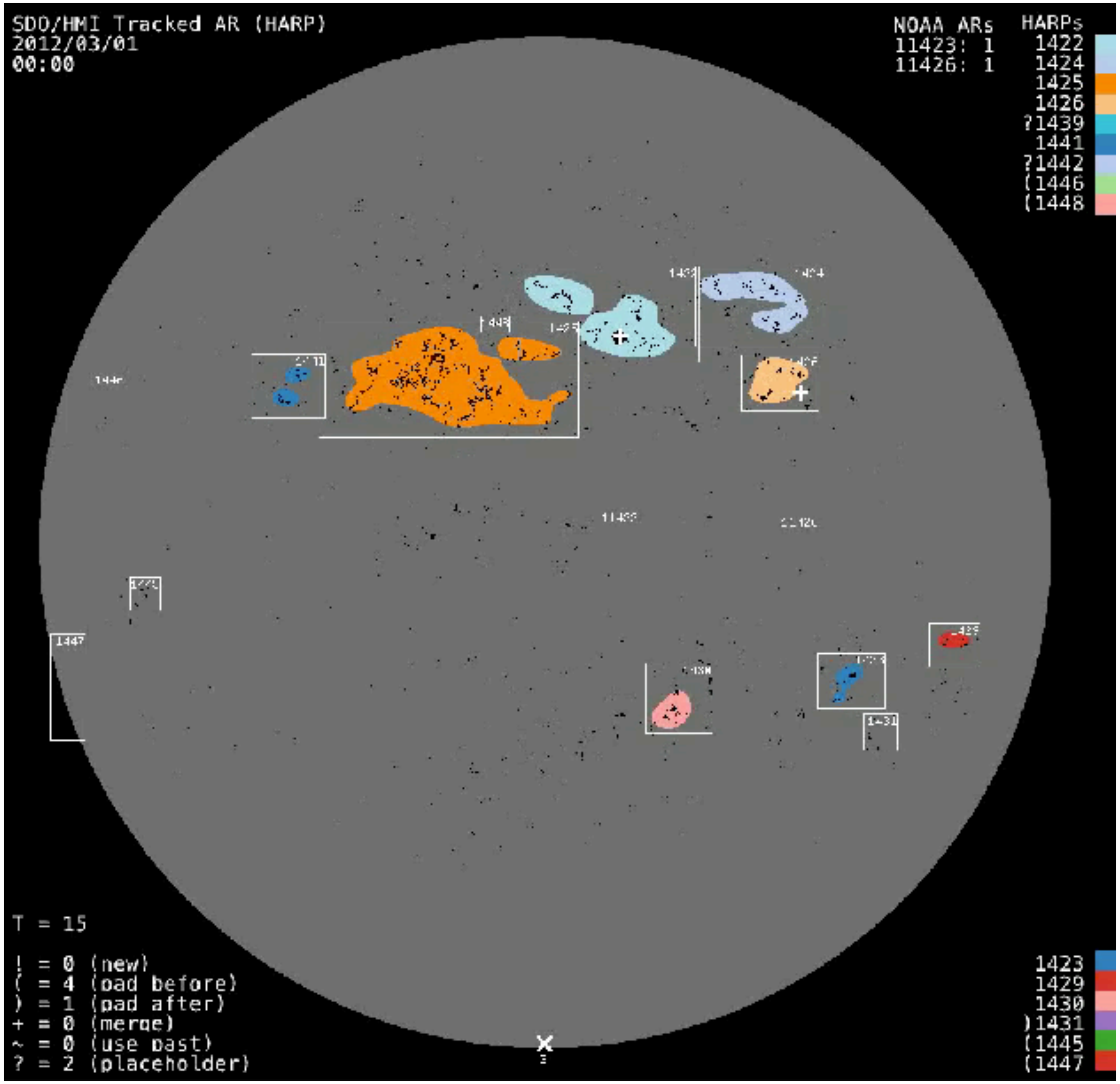

Magnetogram extraction

- Single observation for each SHARP — when flux-weighted centroid closest to CM.

Gaussian smoothing

Interpolate to 360x180 grid

Fit BMR

if sufficiently flux-balanced

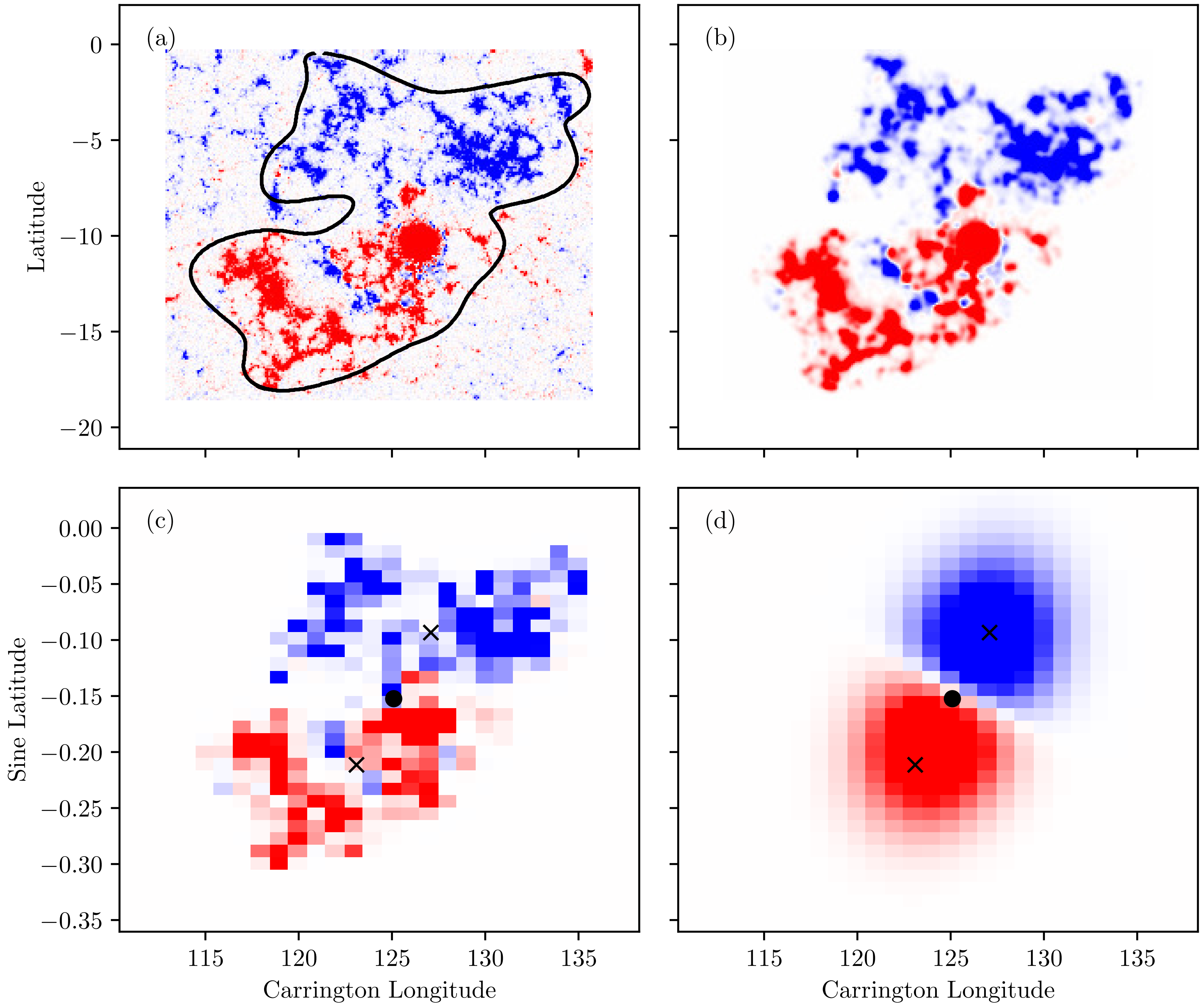

Bipolar approximation

- Fit based on polarity centroids:

$$B(s,\phi) = -B_0 \frac{\phi}{\rho} \exp\left[-\frac{\phi^2 + 2\arcsin^2(s)}{(a\rho)^2}\right]$$

- Rotate to correct location and tilt angle.
- Scale unsigned flux to match.

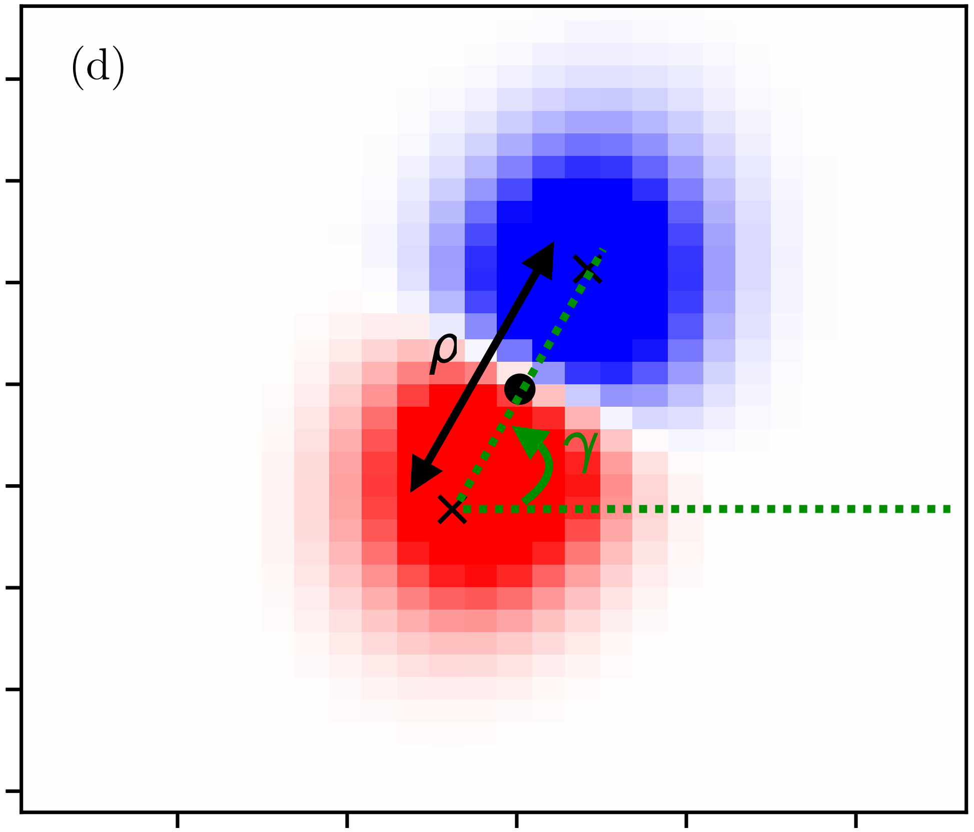

- Parameter *a* controls dipole moment for given flux. Set *a* = 0.56 so axial dipole moment of BMR matches that of original SHARP.

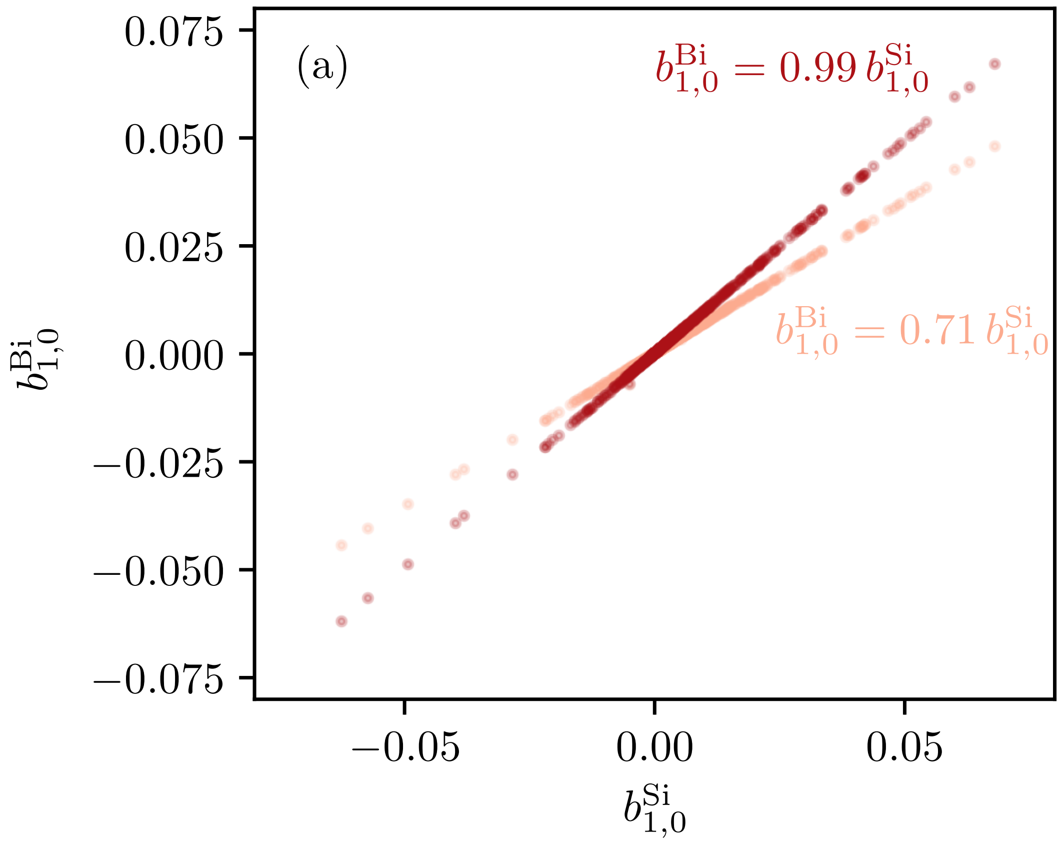

Filtering

- Initially: 3671 regions, total flux 1.4e25 Mx

1. Remove SHARPs with too much flux imbalance.
   [2323 regions, total flux 0.18e25 Mx]
2. Remove SHARPs where separation too small to resolve on computational grid.
   [114 regions, total flux 0.004e25 Mx]
3. Remove repeat observations.
   [143 regions, total flux 0.17e25 Mx]

- Remaining: **1090 regions, total flux 1.0e25 Mx**.

Automated removal of repeats

- Every SHARP is compared with those passing CM between 20-34 days earlier.
- A “repeat” is where an earlier SHARP had more flux in its derotated footprint.

not a repeat
R < 1

repeat
R > 1

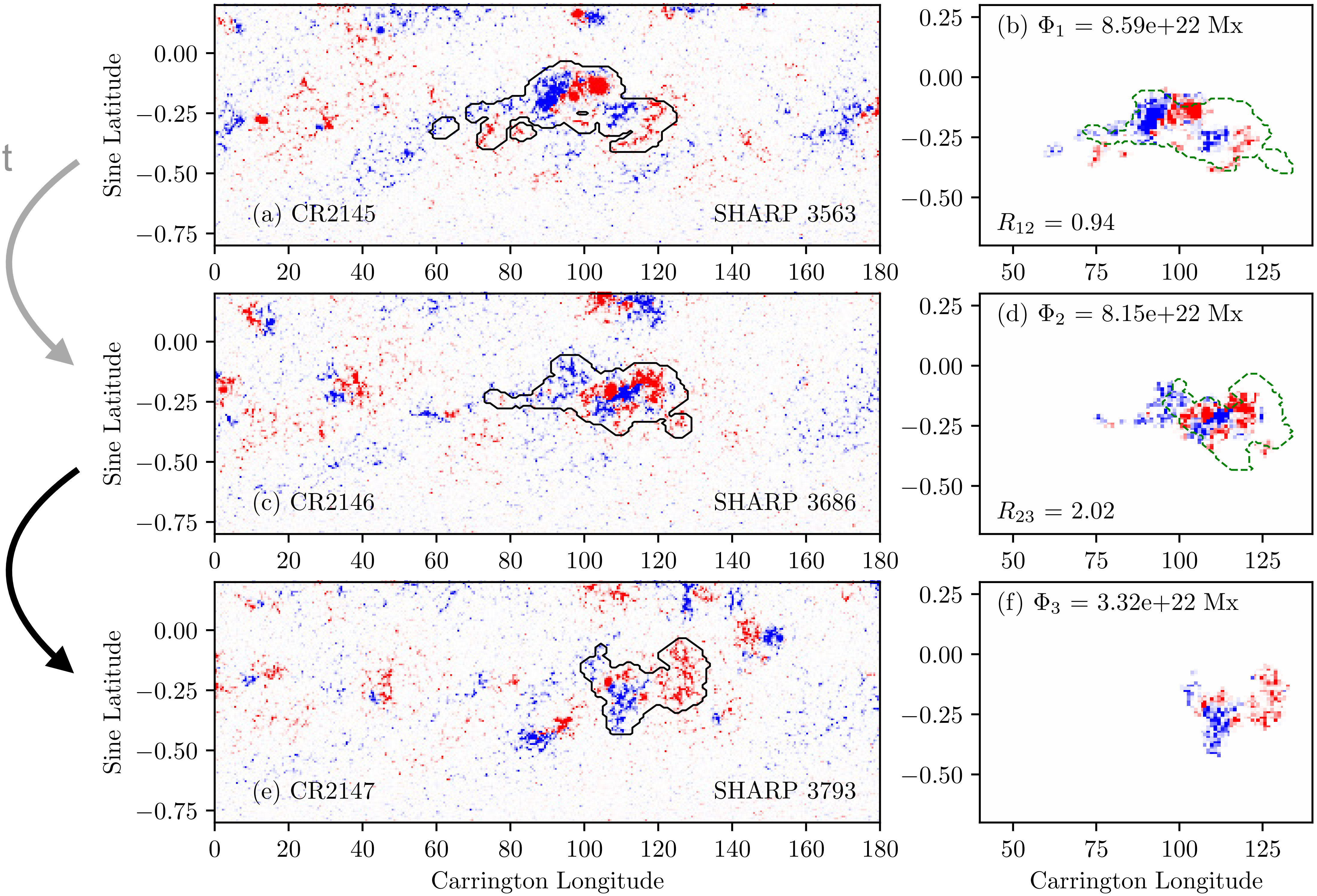

Summary of emergence-time properties

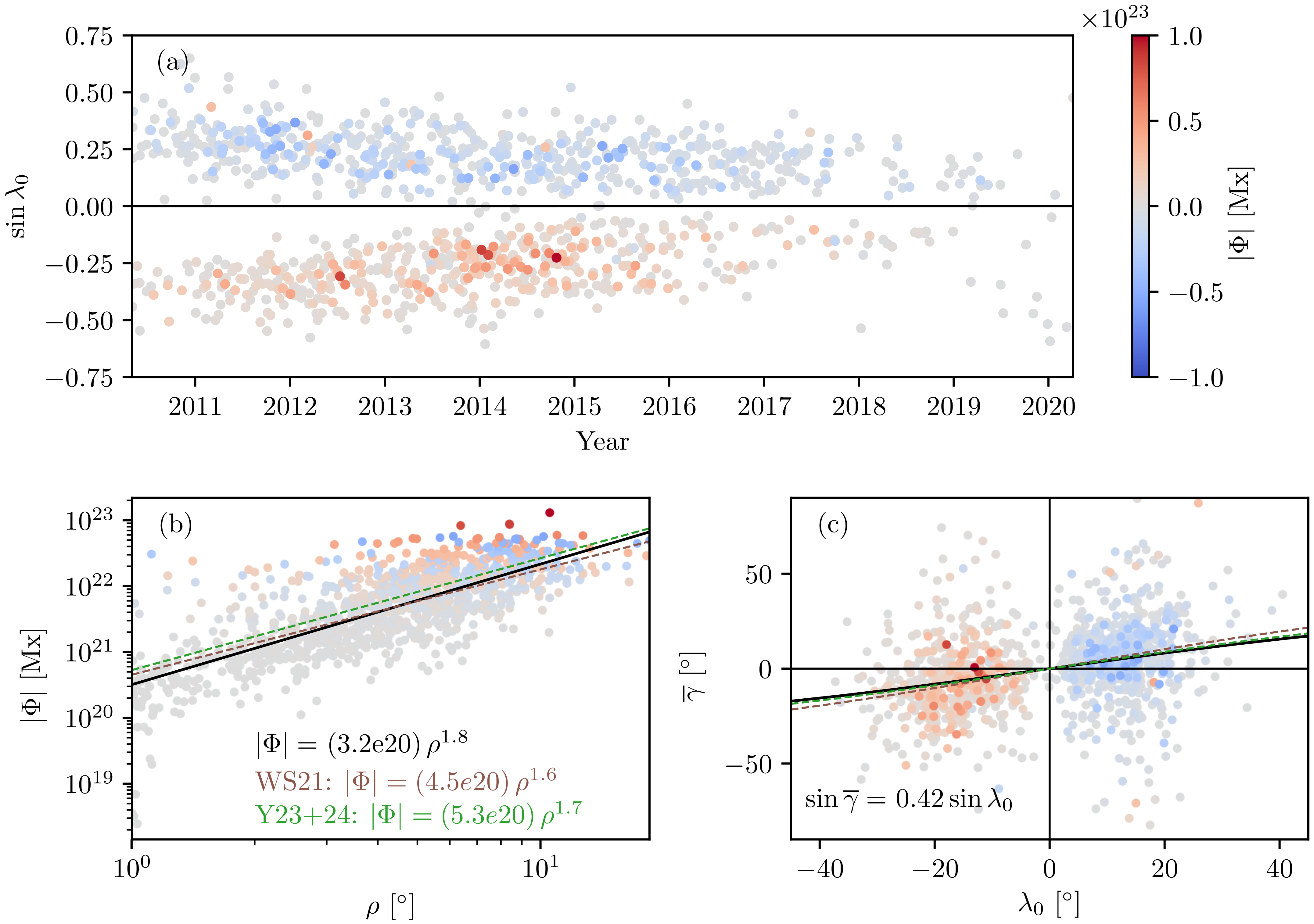

- Database includes predicted final dipole moment from Surface Flux Transport of (a) the BMR and (b) the original SHARP.

Evolution

Surface flux transport model

- To compute the axial dipole moment we only need to evolve the 1D longitude-averaged field:

$$\frac{\partial\overline{B}}{\partial t} = \frac{\partial}{\partial s}\left[\frac{D}{R_\odot^2}(1-s^2)\frac{\partial\overline{B}}{\partial s} - \frac{v_s(s)}{R_\odot}\sqrt{1-s^2}\,\overline{B}\right] \qquad s = \cos\theta$$

supergranular diffusion

meridional flow

$$v_s(s) = D_u s(1-s^2)^{p/2} \quad \left[= D_u \cos\theta \sin^p\theta\right]$$

- Parameters set using full simulation [all SHARPs, initialised with smoothed HMI synoptic map].

$D = 350\,\mathrm{km^2\,s^{-1}}$ $\qquad D_u = 0.041\,\mathrm{km\,s^{-1}}$ $\qquad p = 2.33$

[same profile as Whitbread-Y-Muñoz-J 2018, but faster flow and slower diffusion]

- No exponential decay term [didn't seem to be needed to match observed evolution].

Complete simulation

[here I ran in 2D for illustration]

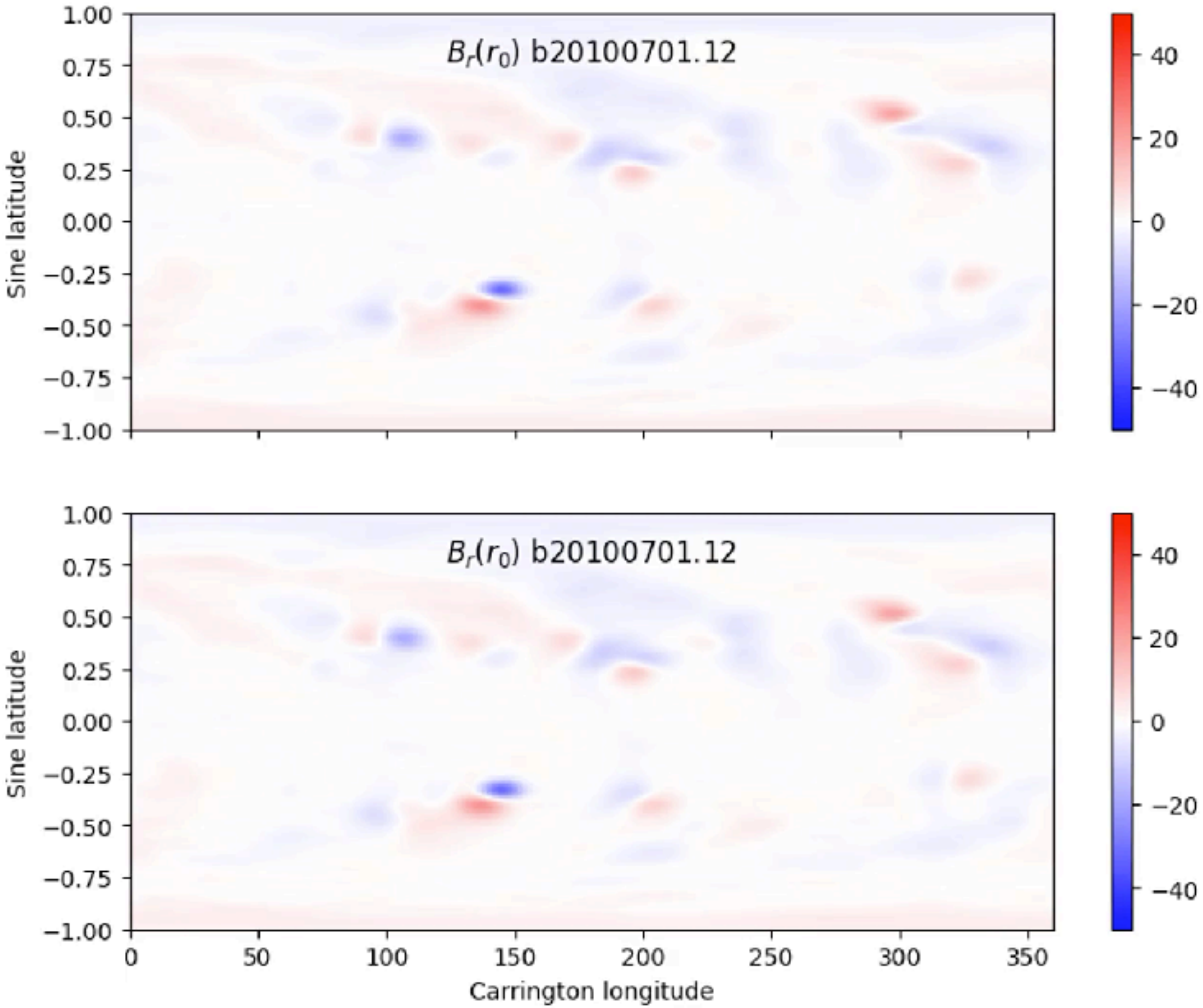

BMRs

SHARPs

Complete simulation

[1D results]

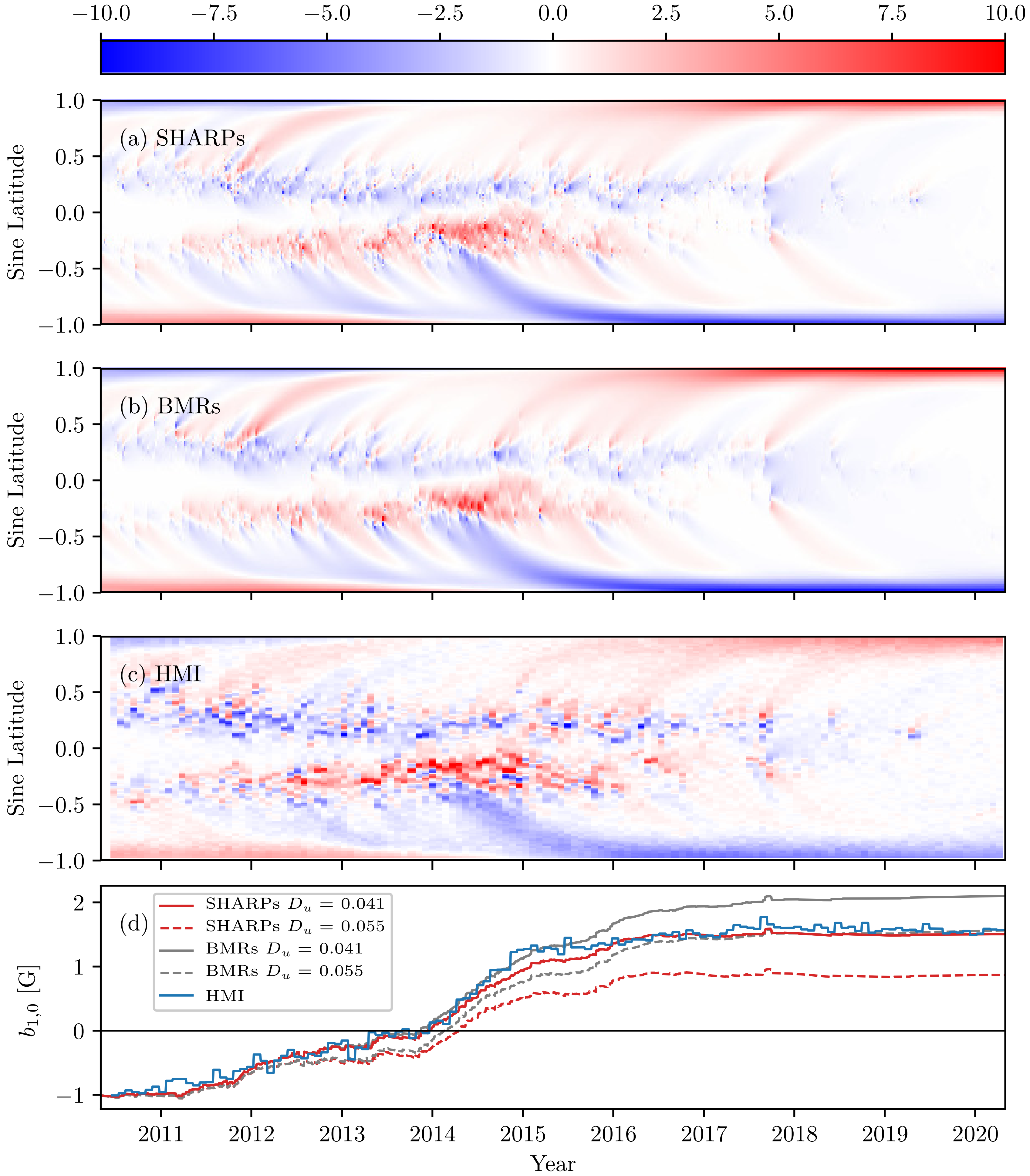

- BMRs overestimate dipole moment by 24%.

Individual evolutions

- Solve with finite-differences for each region individually [10 years to steady state].

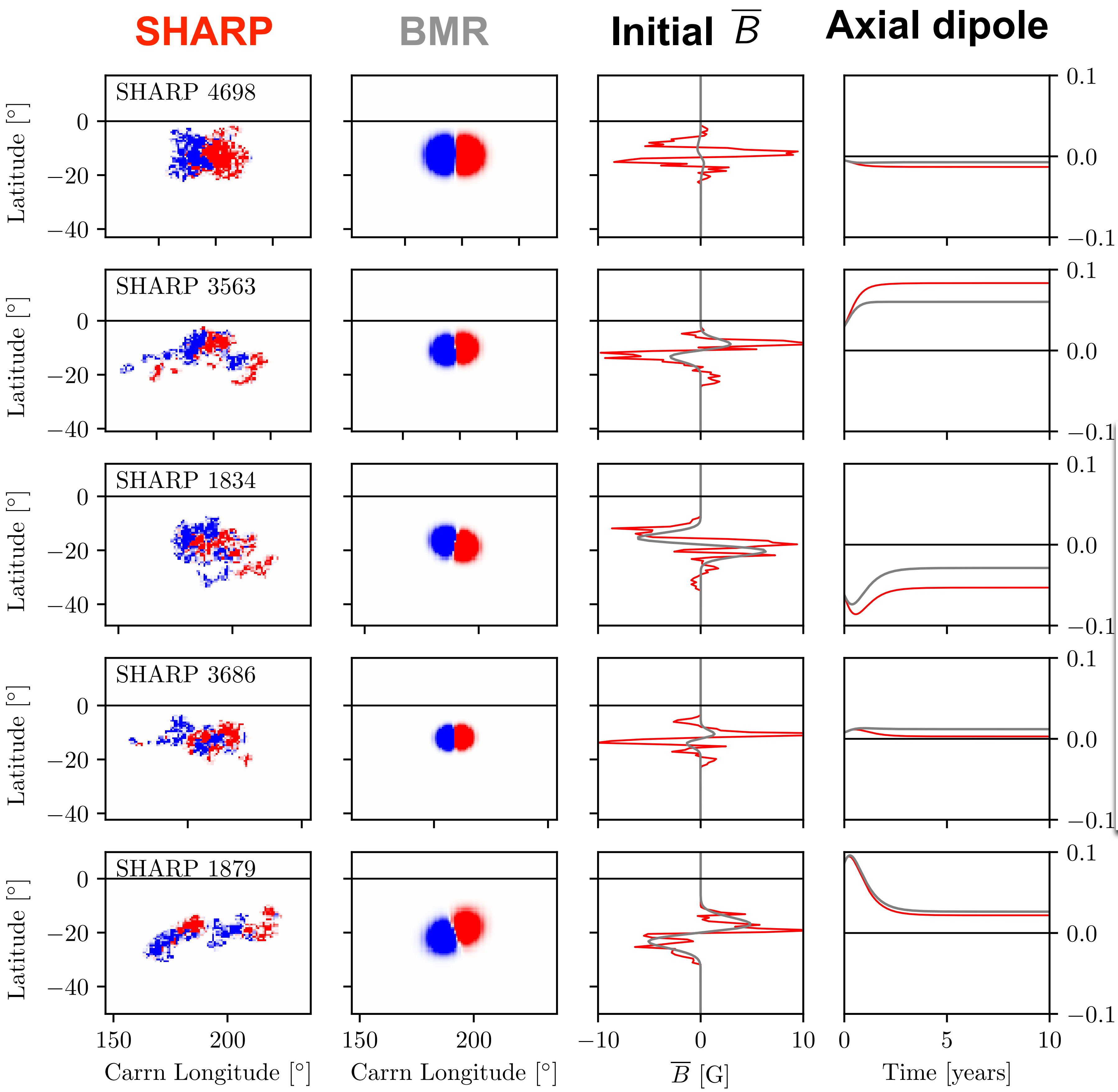

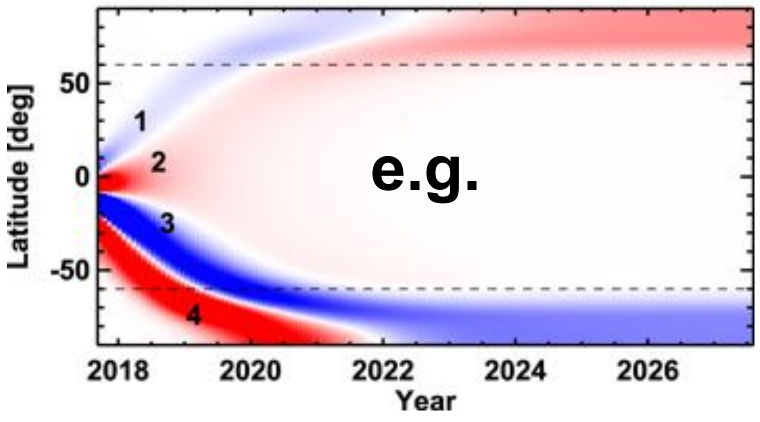

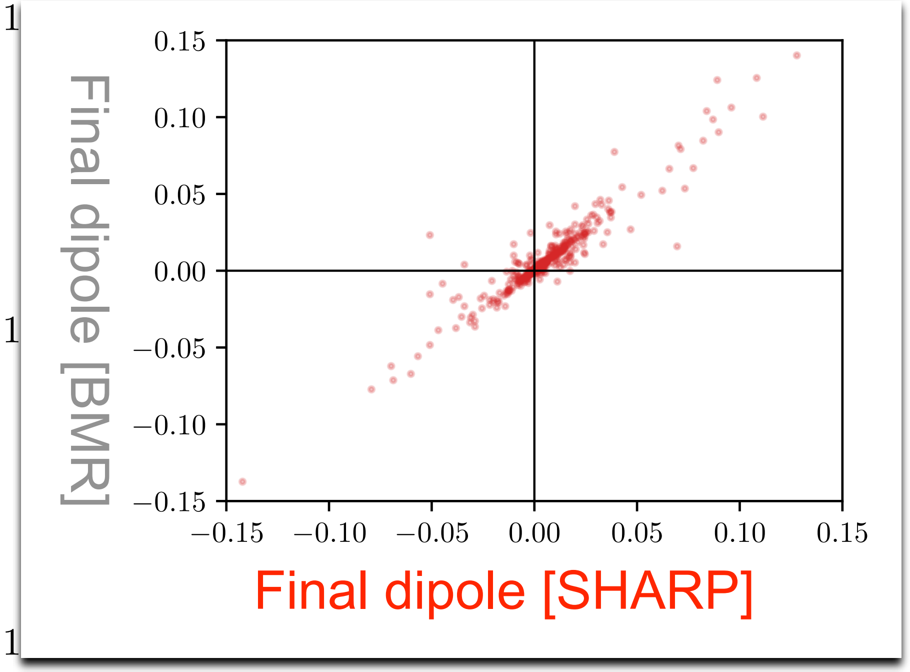

Dipole amplification

- Ratio of final to initial dipole moment [Jiang-Cameron-Schüssler 2014].
- As explained by Petrovay-Nagy-Yeates 2020 this follows a Gaussian in latitude for BMR sources.
- But for SHARPs not all regions fall on the curve:

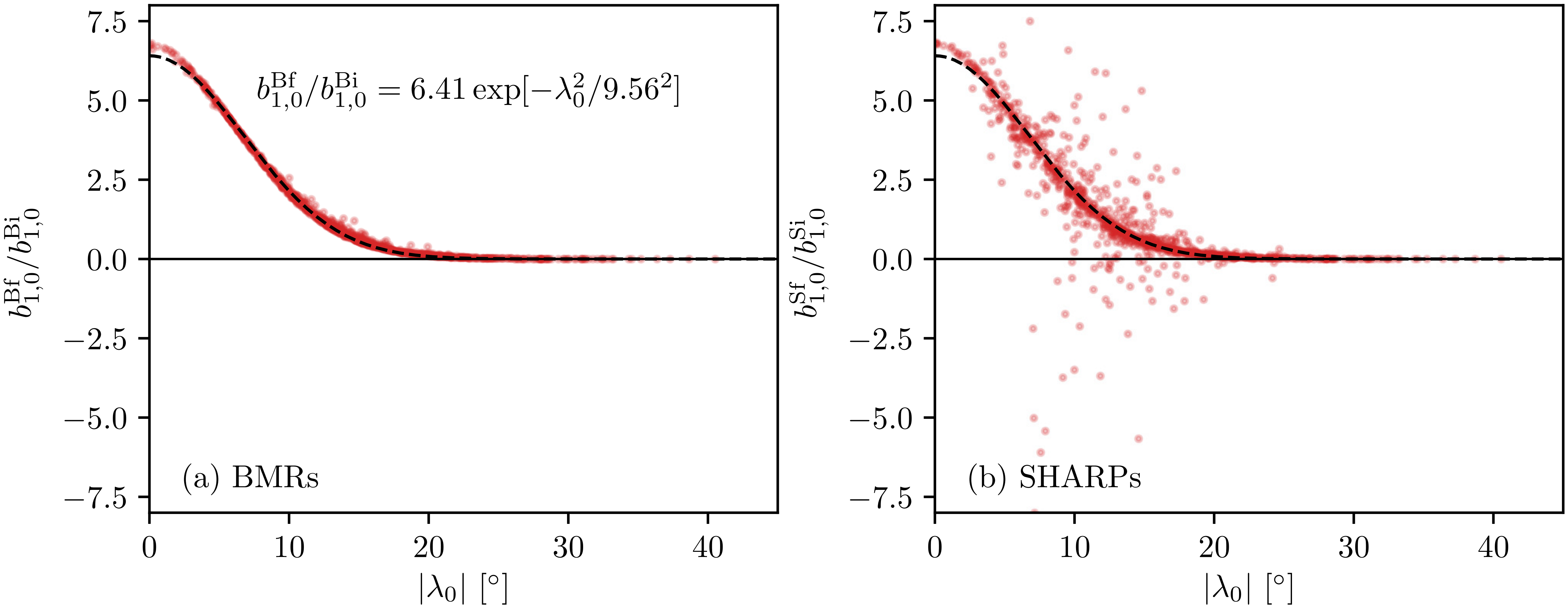

- There are more SHARPs below the curve than above => weaker dipole.
- These are “non-dipolar” regions with enhanced cancellation.

Regions with the largest discrepancy

following polarity more diffuse [cf. Iijima-Hotta-Imada 2019]

more complex initial shape [cf. Jiang et al 2019]

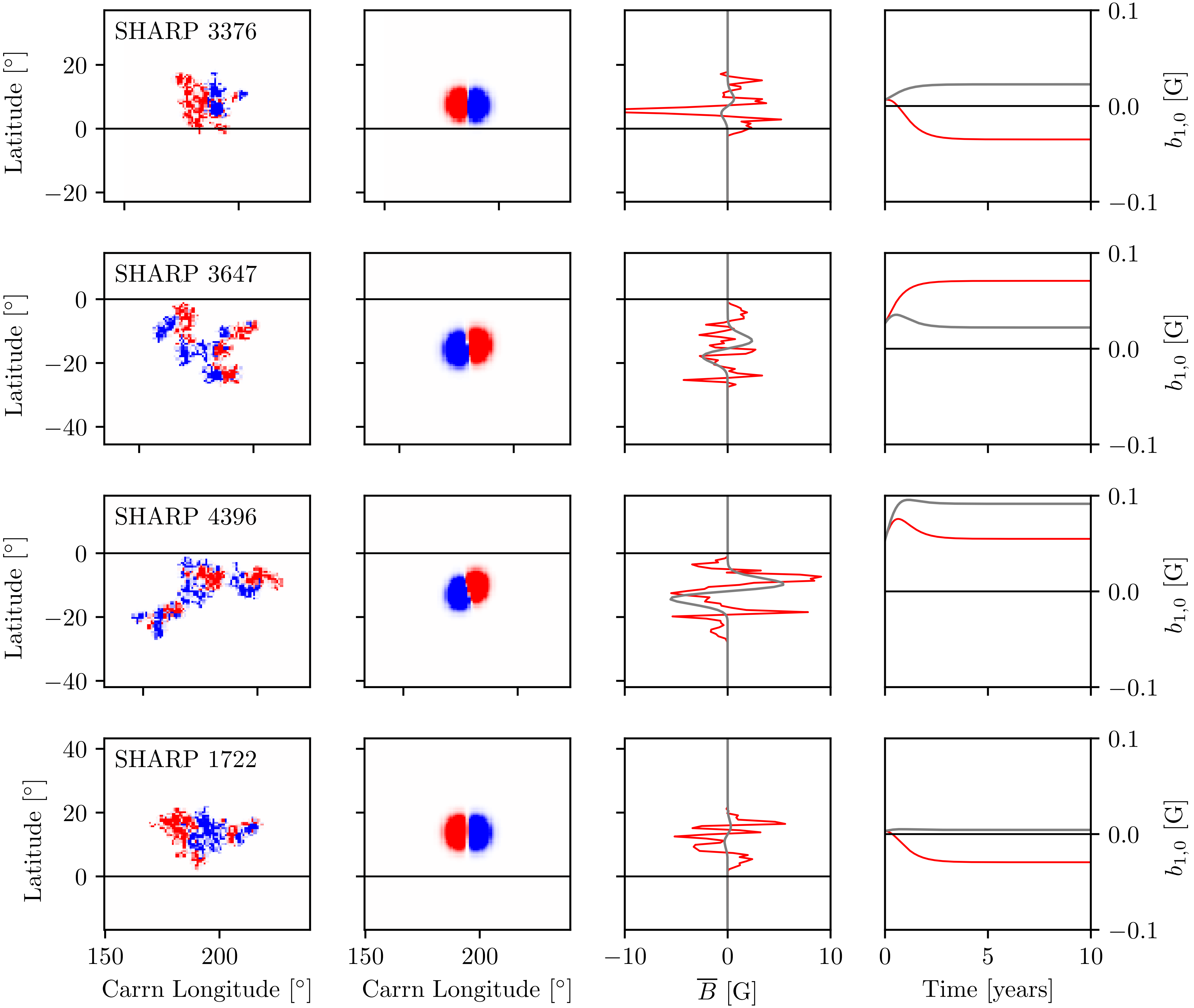

Reflections

- Suggests that active region inflows are not the cause of the overestimate of dipole from BMRs.
  [inflows may be accounted for already with my faster meridional flow]

- If SHARPs are used, dipole reverses at correct time even without decay term.
  [cf. Petrovay-Talafha 2019]

- Reducing the tilt angles has the same effect as slowing down the meridional flow:

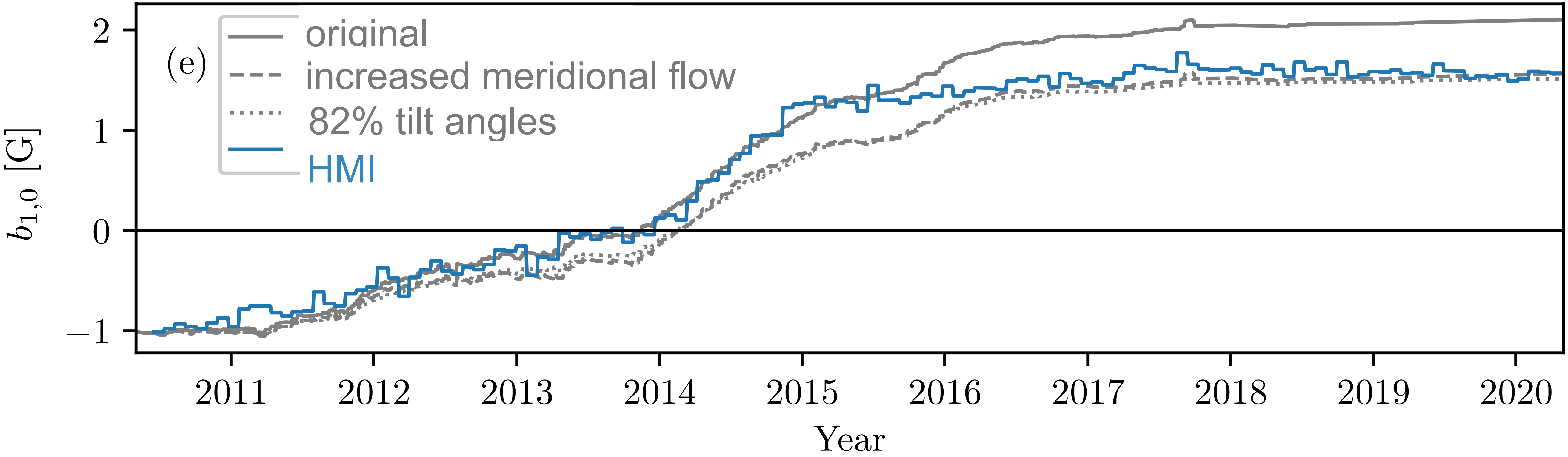

Driving Coronal Simulations

[work in progress]

Magnetofrictional model

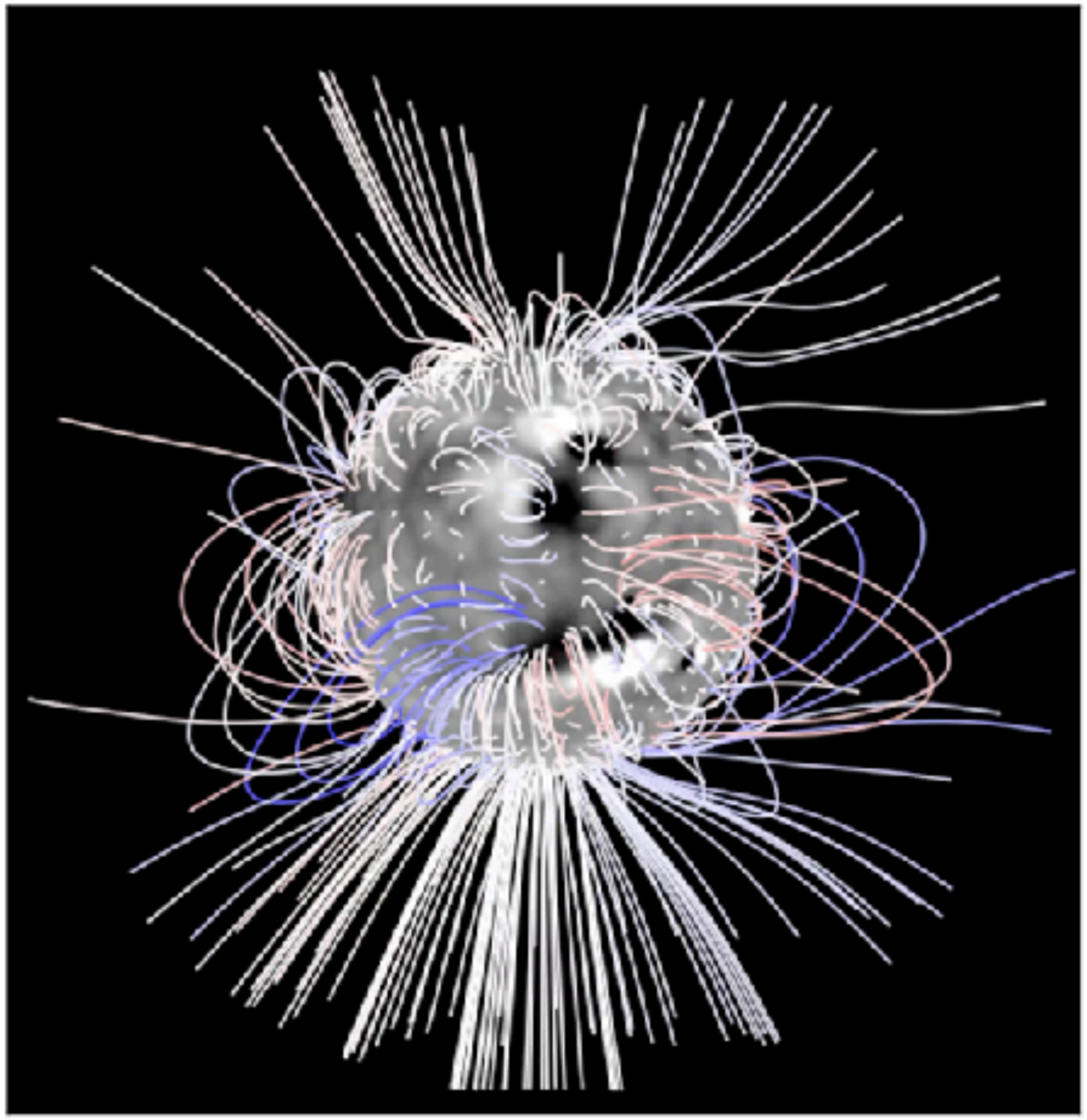

- Quasi-static evolution but preserving magnetic topology with induction equation [van Ballegooijen-Priest-Mackay 2000; Yeates 2014].

$$\boldsymbol{B} = \nabla \times \boldsymbol{A}$$

$$\frac{\partial \boldsymbol{A}}{\partial t} = \boldsymbol{v} \times \boldsymbol{B} - \eta \nabla \times \boldsymbol{B}$$

$$\boldsymbol{v} = \frac{(\nabla \times \boldsymbol{B}) \times \boldsymbol{B}}{\nu(B^2)} + v_{\text{out}} \left(\frac{r}{R_{ss}}\right)^{11.5} \hat{\boldsymbol{r}}$$

- Boundary conditions:
  - zero gradient on $r = R_{ss} = 2.5 R_\odot$
  - on $r = R_\odot$ set $\frac{\partial \boldsymbol{A}_h}{\partial t} = \underbrace{\boldsymbol{v}_h \times (B_r \hat{\boldsymbol{r}})}_{\text{differential rotation}} - \underbrace{D \nabla \times (B_r \hat{\boldsymbol{r}})}_{\text{supergranular diffusion}} + \underbrace{\boldsymbol{E}_{em}}_{\text{emergence}}$

- Previous simulations were driven by emergence of analytical bipoles [e.g. Yeates-Mackay-van Ballegooijen 2008].

How to emerge SHARPs

1. Compute local **A** on photosphere for the new region.

e.g.

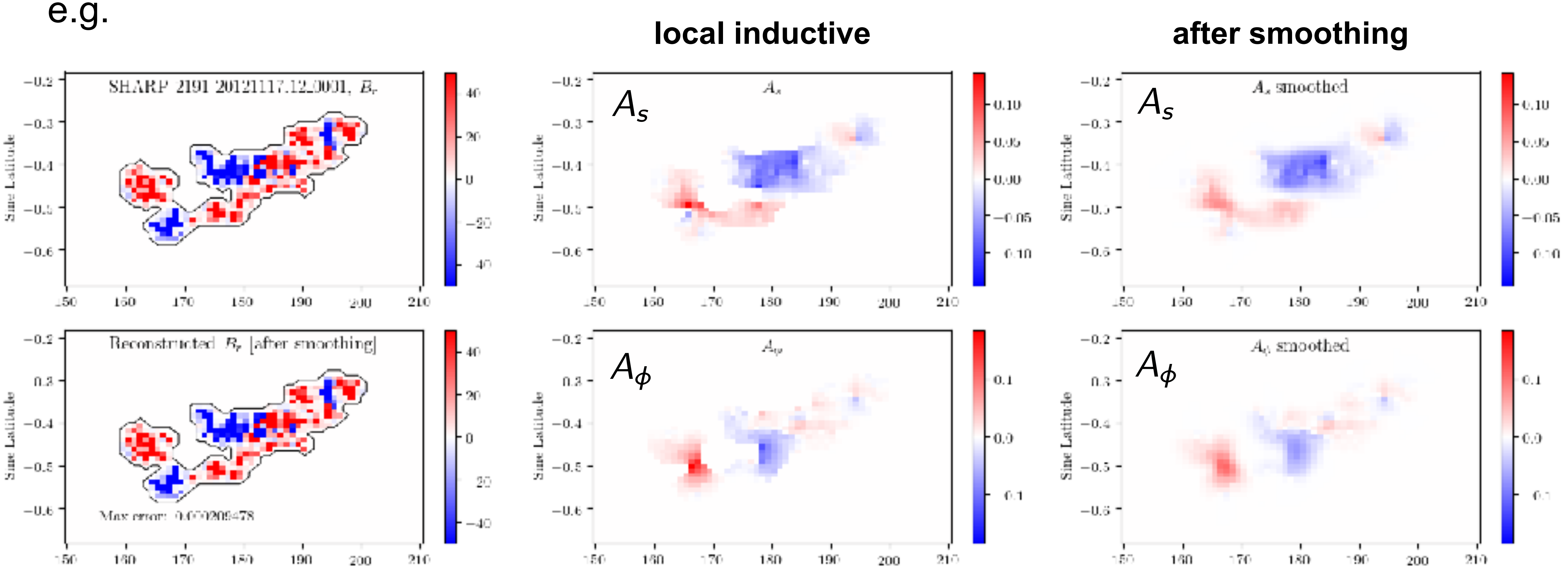

- “Local inductive” method:

  minimize $\sum_{D} |\boldsymbol{A}|^2$ subject to $\hat{\boldsymbol{r}} \cdot \nabla \times \boldsymbol{A} = B_r$ with boundary condition $\boldsymbol{A} \times \boldsymbol{n}\big|_{\partial D} = \boldsymbol{0}$.

- Jumps in ***A.n*** are then removed by applying a “curl-free smoothing” $\dfrac{\partial \boldsymbol{A}}{\partial t} = \nabla(\nabla \cdot \boldsymbol{A})$.

Why is the localization necessary?

- Avoids spurious energization of the coronal field outside the emergence region.

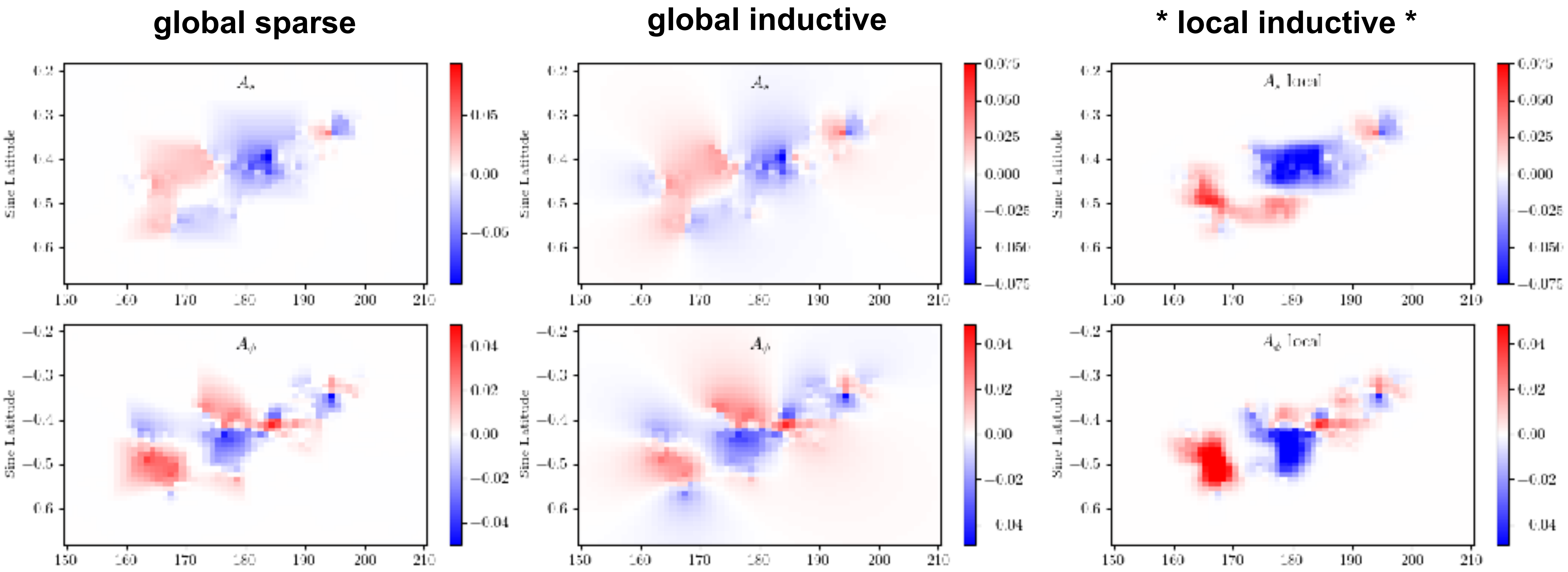

global sparse

global inductive

*** local inductive ***

cf. Fisher et al (ApJS) 2020 - electric field inversion techniques.

cf. Yeates 2017 - sparse electric fields.

How to emerge SHARPs

2. Apply steady electric field ***A***/dt for fixed emergence time - e.g. dt=12 hours.

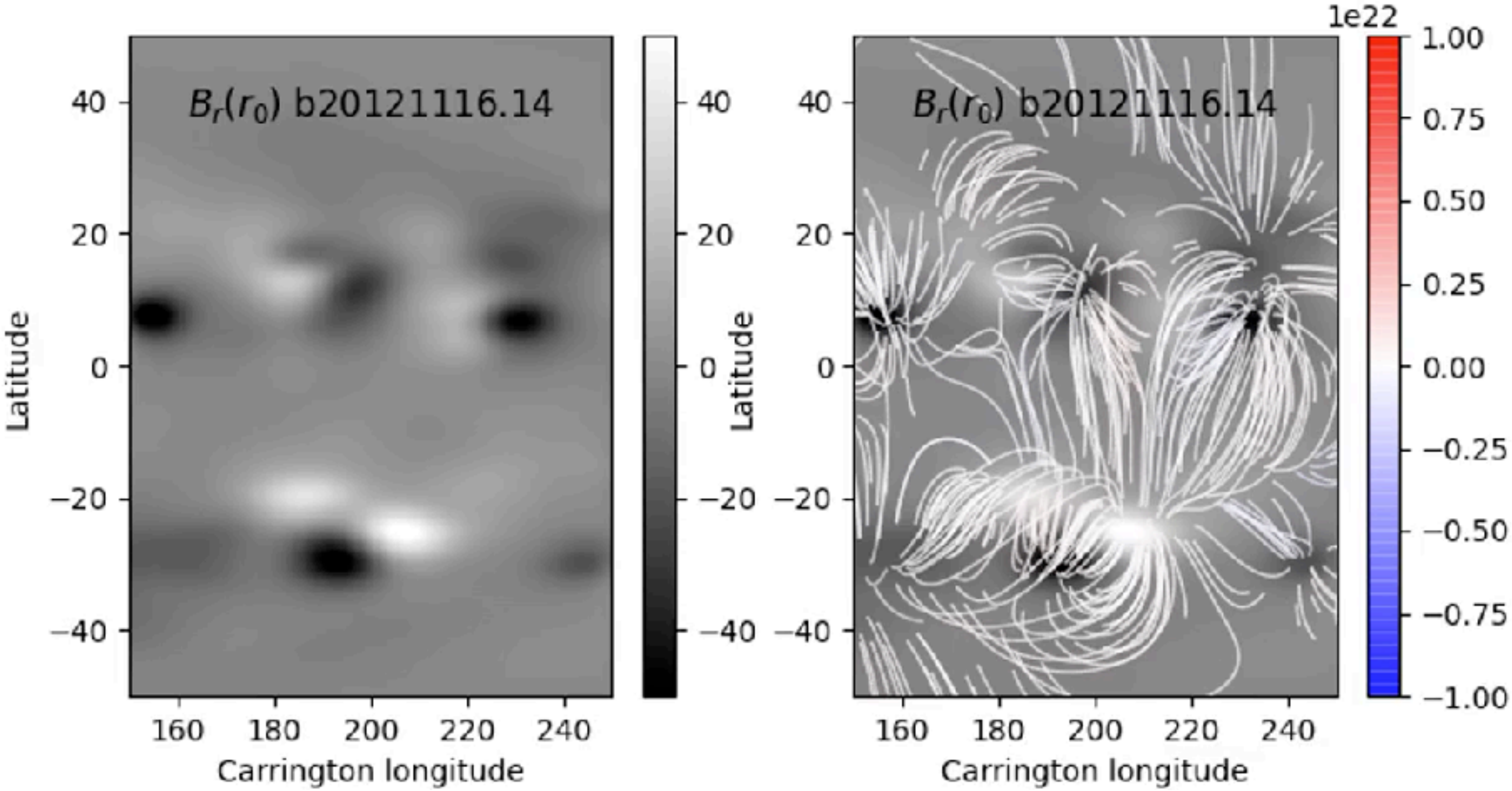

- **Still testing**: addition of twist informed by HMI measurements of $\alpha = \dfrac{j_r}{B_r}$

Full simulation [preliminary]

- Longitude averages of B_r.

$r = R_\odot$

SHARPs

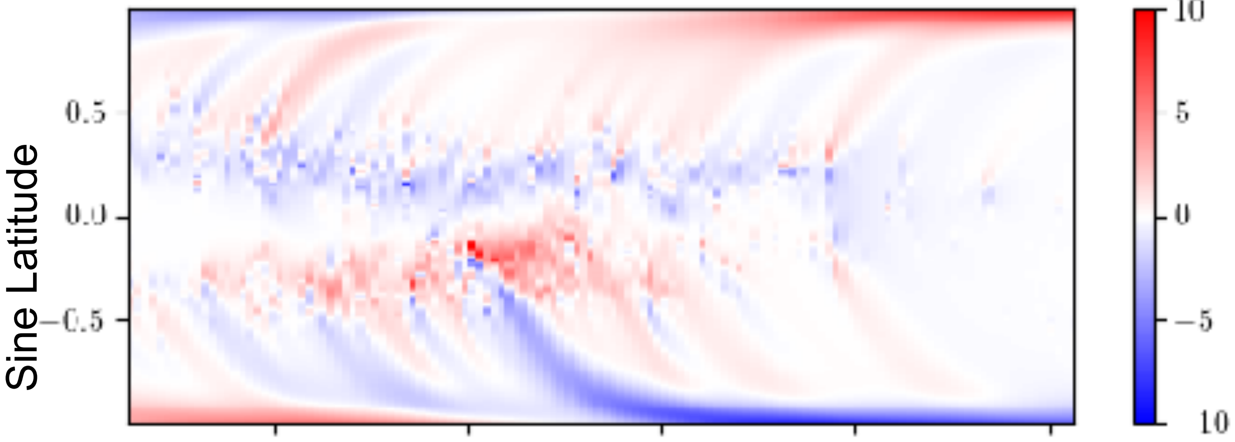

BMRs [82% tilt]

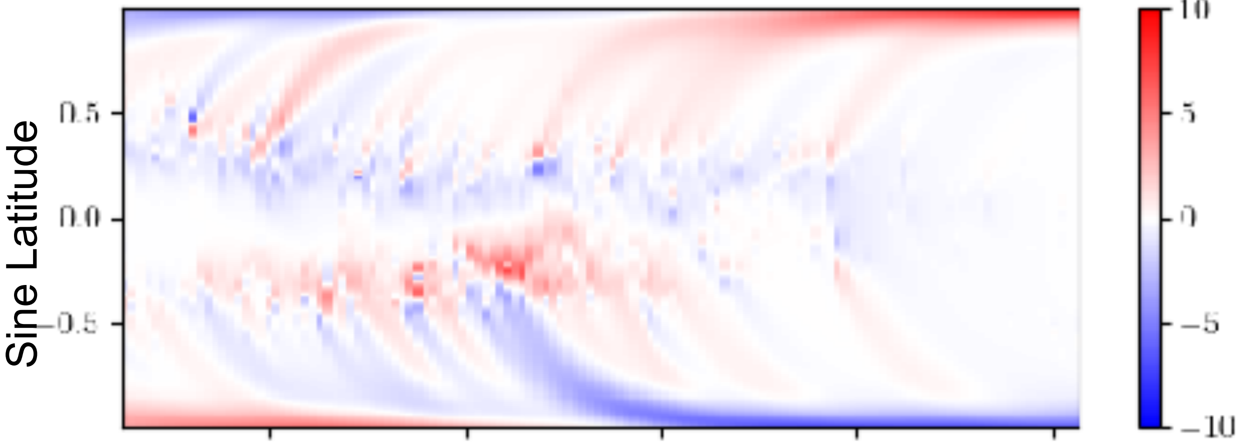

HMI

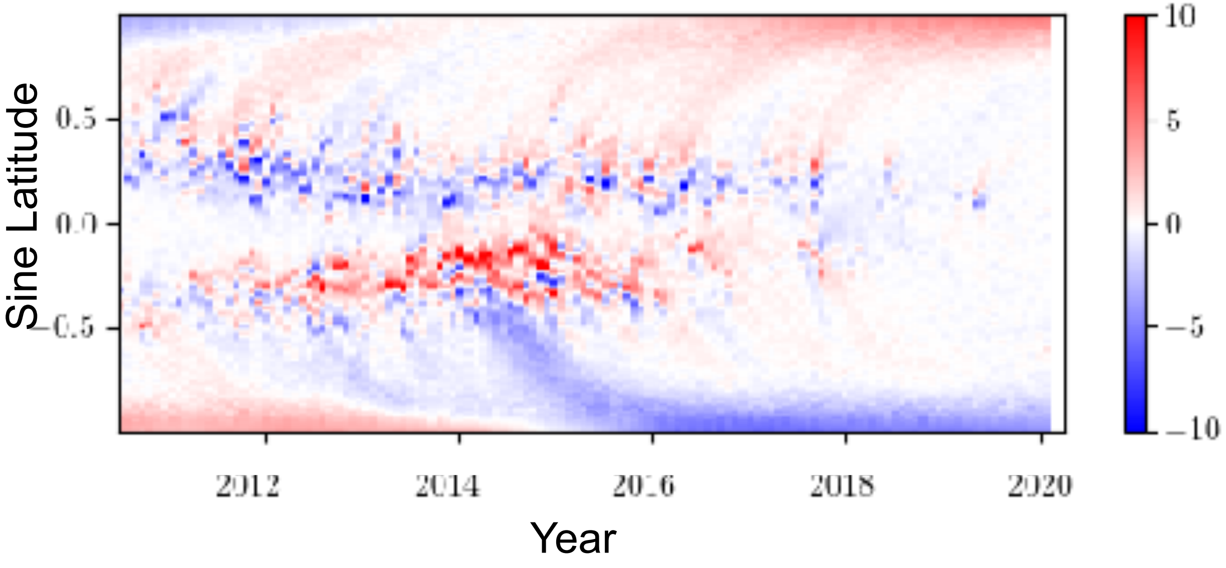

$r = 2.5R_\odot$

SHARPs+MF

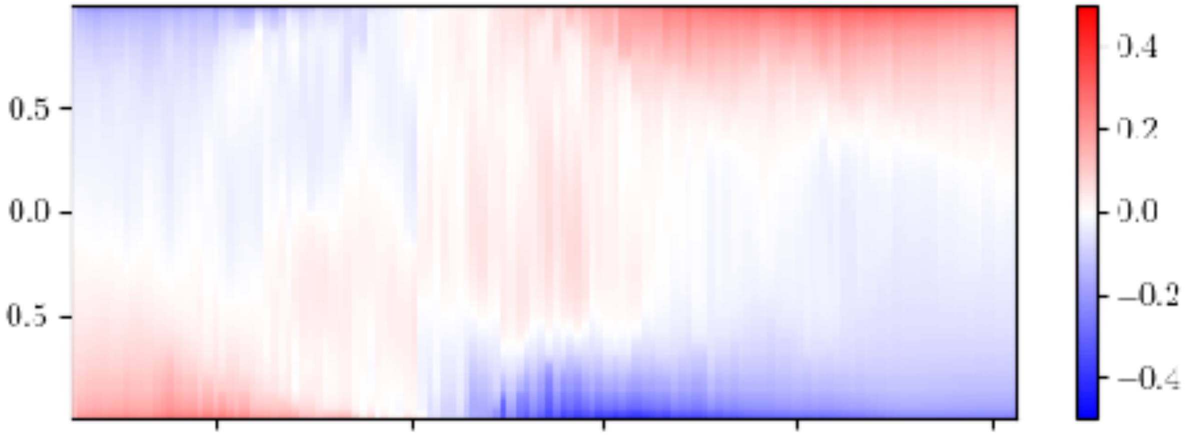

BMRs [82% tilt] + MF

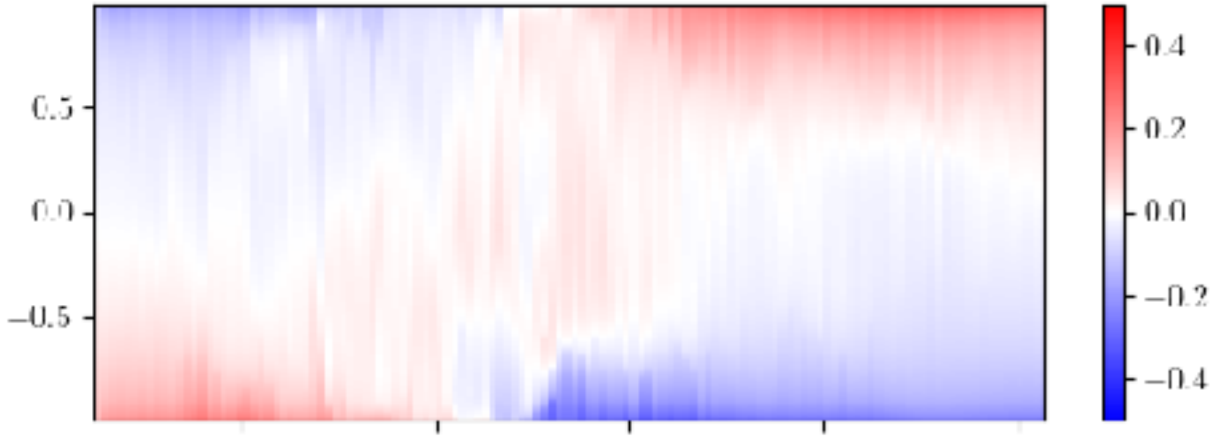

HMI+PFSS

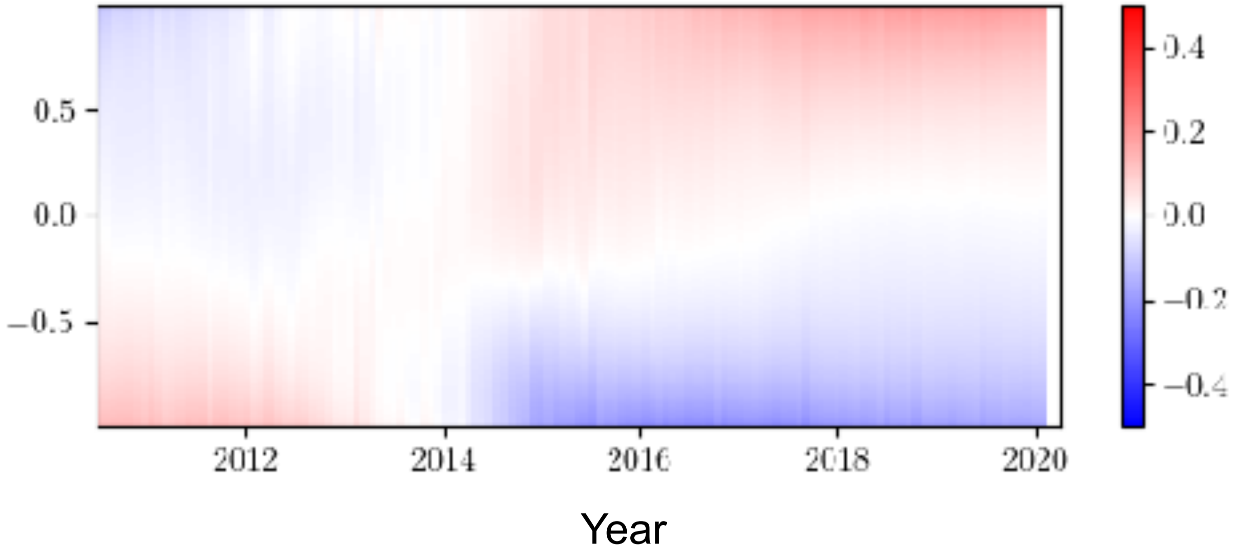

Conclusion

- Automated database of Bipolar Magnetic Regions from HMI/SHARPs.
- Flux transport model with BMRs overestimates end-of-cycle dipole by 24% compared to model with original SHARP shapes.

A.R. Yeates, How good is the bipolar approximation of active regions for surface flux transport?, *Solar Physics* **295**, 119 (2020)

- Python code for extracting database: https://github.com/antyeates1983/sharps-bmrs
- Ready-prepared file: https://doi.org/10.7910/DVN/1Z7YMT (Harvard Dataverse) for May 2010 to April 2020.
- **Ongoing work** [with postdoc Prantika Bhowmik]: magnetofrictional simulations of Cycle 24 — how does coronal field depend on
  - bipolar approximation?
  - emergence electric field?
  - twisting of emerging regions?

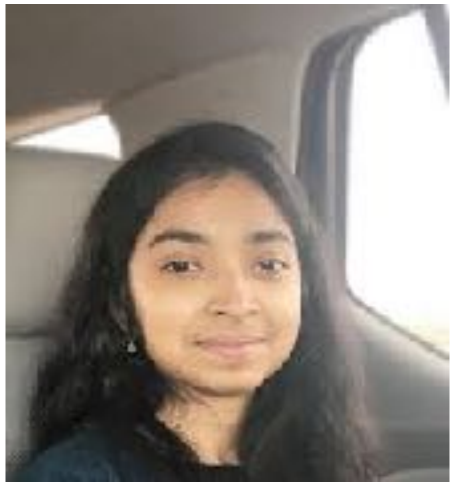

Science and Technology Facilities Council

The End!